Analysis of Light–Matter Systems

by

Mohamed El Mandouh

A thesis
presented to the University of Waterloo
in fulfillment of the
thesis requirement for the degree of
Master of Mathematics
in
Applied Math (Quantum Information)

Waterloo, Ontario, Canada, 2021

© Mohamed El Mandouh 2021

Author's Declaration

I hereby declare that I am the sole author of this thesis. This is a true copy of the thesis, including any required final revisions, as accepted by my examiners.

I understand that my thesis may be made electronically available to the public.

Abstract

In this thesis we introduce the simplest model of a two–level system coupled to a single mode of an optical cavity, called the Jaynes–Cummings model. This model is then extended to an ensemble of identical two–level systems and is studied in more detail, also known as the Tavis–Cummings model. This model is intractable, but we show that by a clever but simple choice of basis one can reduce the dimensionality of the Tavis–Cumming system. We then demonstrate the effectiveness of this reduction by calculating interesting statistics of the system, and simulating large ensembles of two–level systems which were not practical before. Finally, we examine some dynamics of the Tavis–Cummings model in the presence of photon losses, and introduce a method for population transfer by modulating TLS–cavity interaction strength.

Acknowledgements

I would like to thank everyone in the Cory group for all the engaging discussions and for the incredible breadth of topics in our weekly meetings which greatly broadened my horizons. I would especially like to thank Andrew Stastiuk, Lane Gunderman, and Troy Borneman for all the fun physics and non–physics related discussions. Finally, I would like to thank my supervisor David Cory for all the interesting problems, patience and guidance.

Table of Contents

List of Figures

Chapter 1

Introduction

Through the interaction of a single two–level system (spins [49], superconducting qubits [35], and neutral atoms [36]) with a single mode of an optical cavity, coherent exchange of a quantum excitation can be realized. The study of light–matter interactions of this form is thus called cavity quantum electrodynamics (cQED). The Tavis–Cummings model was introduced in quantum optics to describe the behaviour of an identical ensemble two–level systems interacting with a single mode of the electromagnetic field. The Tavis–Cummings model is of current interest as it can be used for the implementation of many quantum information methods. In this section we begin by introducing a simpler model of a single two–level system coupled to a single cavity mode, called the Jaynes–Cummings model. Then we introduce the Tavis–Cummings model, and describe regimes in which the model is exactly solvable.

1.1 Jaynes–Cummings Model

The system of interest in this thesis is that of many two–level systems coupled to a single mode of the cavity, also known as the Tavis–Cummings model. We begin however by considering the simplest case of one two–level system (TLS) coupled to a single mode of the cavity, known as the Jaynes–Cummings model.

1.1.1 A Single Two–Level System in a Cavity

The Hamiltonian of a single two–level system in an optical cavity is the sum of three terms

$$\hat{\mathcal{H}} = \hat{\mathcal{H}}_{\text{tls}} + \hat{\mathcal{H}}_{\text{c}} + \hat{\mathcal{H}}_{\text{int}}, \tag{1.1}$$

where $\hat{\mathcal{H}}_{\text{tls}}$, $\hat{\mathcal{H}}_{\text{c}}$, and $\hat{\mathcal{H}}_{\text{int}}$ describe the TLS, the cavity subsystem and the TLS–cavity interaction, respectively. The two levels of the TLS are the ground state $|g\rangle$ and excited state $|e\rangle$, such that (we set $\hbar = 1$ all through this text)

$$\hat{\mathcal{H}}_{\text{tls}} = \frac{\omega_{\text{tls}}}{2}\hat{\sigma}_z, \tag{1.2}$$

where ω_{tls} is the frequency of the TLS. While $\hat{\sigma}_z$ is the Pauli z spin operator, which can also be understood as the population difference between ground and excited state. $\hat{\sigma}_z$ is written in terms of the ground and excited state as

$$\hat{\sigma}_z = |g\rangle\langle g| - |e\rangle\langle e|\,. \tag{1.3}$$

In addition, the spin operators responsible for the transition between the ground and excited state are the raising $\hat{\sigma}_+$ and lowering operator $\hat{\sigma}_-$. The raising and lowering operators are written as

$$\hat{\sigma}_+ = |e\rangle\langle g|\,, \tag{1.4}$$

$$\hat{\sigma}_- = |g\rangle\langle e|\,. \tag{1.5}$$

These operators satisfy the Pauli spin–1/2 Lie algebra

$$[\hat{\sigma}_-, \hat{\sigma}_+] = -2\hat{\sigma}_z, \tag{1.6}$$

$$[\hat{\sigma}_-, \hat{\sigma}_z] = \hat{\sigma}_-. \tag{1.7}$$

On the other hand, we can describe the energy of the cavity in the second quantization formalism [30]

$$\hat{\mathcal{H}}_{\text{c}} = \omega_{\text{c}}\hat{a}^\dagger\hat{a}, \tag{1.8}$$

where ω_c is the frequency of the cavity mode. While $\hat{a}^\dagger$ and $\hat{a}$ are the creation and annihilation operators satisfying

$$[\hat{a}, \hat{a}^\dagger] = 1, \tag{1.9}$$

$$\hat{a}\,|n\rangle = \sqrt{n}\,|n-1\rangle\,, \tag{1.10}$$

$$\hat{a}^\dagger\,|n\rangle = \sqrt{n}\,|n+1\rangle\,. \tag{1.11}$$

The $\hat{a}^\dagger\hat{a}$ term can be understood as the number (photon) counting operator.

Finally, the energy of the interaction between the TLS and the cavity is given by the electric dipole moment $E = \vec{d}\cdot\vec{E}$. The quantized Hamiltonian description is then given by [43]

$$\hat{\mathcal{H}}_{\text{int}} = g(\hat{\sigma}_+ + \hat{\sigma}_-)(\hat{a}^\dagger + \hat{a}), \tag{1.12}$$

where g is coupling strength between the TLS and the cavity. The interaction Hamiltonian consists of two terms, the "co–rotating" term $\hat{\sigma}_+\hat{a} + \hat{\sigma}_-\hat{a}^\dagger$ and the "counter–rotating" term $\hat{\sigma}_+\hat{a}^\dagger + \hat{\sigma}_-\hat{a}$. The counter-rotating term can be neglected in the regime $g \ll \omega_{\text{tls}},\ \omega_{\text{c}}$, also known as the rotating–wave approximation (RWA). In the regimes where the RWA holds the full Jaynes–Cummings Hamiltonian [30] is

$$\hat{\mathcal{H}} = \frac{\omega_{\text{tls}}}{2}\hat{\sigma}_z + \omega_{\text{c}}\hat{a}^\dagger\hat{a} + g(\hat{\sigma}_+\hat{a} + \hat{\sigma}_-\hat{a}^\dagger). \tag{1.13}$$

In the presence of photon loss (cavity decay) with decay rate κ, and atomic decay (spontaneous emission) with decay rate γ, the RWA holds in two regimes, the *weak–coupling* and *strong–coupling* regimes. The weak–coupling regime is characterized by $g \ll \omega_{\text{tls}}, \omega_{\text{c}}, \kappa, \gamma$ [50]. Meanwhile, the strong–coupling regime is characterized by $\gamma, \kappa \ll g \ll \omega_{\text{tls}}, \omega_{\text{c}}$, where the coupling strength g is much larger than the decay rates of the cavity and the TLS as to fully realize coherent excitations swap between the cavity and TLS [32]. The RWA approximation breaks down in the *ultra–strong* regime and beyond, that is for $g \gg \omega_{\text{tls}}, \omega_{\text{c}}$.

1.1.2 Jaynes–Cummings Hamiltonian

Notice that in the Jaynes–Cummings Hamiltonian (1.26)

$$\hat{\mathcal{H}} = \frac{\omega_{\text{tls}}}{2}\hat{\sigma}_z + \omega_{\text{c}}\hat{a}^\dagger\hat{a} + g(\hat{\sigma}_+\hat{a} + \hat{\sigma}_-\hat{a}^\dagger), \tag{1.14}$$

the interaction term only causes transitions between $|e\rangle\,|n\rangle$ and $|g\rangle\,|n+1\rangle$. Also, one notices that the excitation number $\hat{N} = \hat{a}^\dagger\hat{a} + \frac{1}{2}\hat{\sigma}_z$ is a constant of motion, that is

$$\left[\hat{N}, \hat{\mathcal{H}}_{\text{int}}\right] = 0. \tag{1.15}$$

This greatly simplifies our analysis of the system, since we only need to solve for just one particular value n of $\hat{N}$. In other words, the Jaynes–Cummings Hamiltonian can be written in a block–diagonal basis of $\hat{N}$

$$\hat{\mathcal{H}} = \begin{bmatrix} \hat{\mathcal{H}}_0 & 0 & 0 & 0 & \cdots & \cdots & \cdots \\ 0 & \hat{\mathcal{H}}_1 & 0 & 0 & \ddots & \ddots & \ddots \\ 0 & 0 & \hat{\mathcal{H}}_2 & 0 & \ddots & \ddots & \ddots \\ \vdots & \ddots & \ddots & \ddots & \ddots & \ddots & \ddots \\ \vdots & \ddots & \ddots & 0 & \hat{\mathcal{H}}_n & 0 & \ddots \\ \vdots & \ddots & \ddots & \ddots & \ddots & \ddots & \ddots \end{bmatrix}. \tag{1.16}$$

Each block $\hat{\mathcal{H}}_n$ takes the form

$$\hat{\mathcal{H}}_n = \begin{bmatrix} \frac{\Delta}{2} & g\sqrt{n+1} \\ g\sqrt{n+1} & -\frac{\Delta}{2} \end{bmatrix}, \tag{1.17}$$

where $\Delta = \omega_{\text{tls}} - \omega_{\text{c}}$ is the TLS–cavity detuning. The eigenstates of the Jaynes–Cummings Hamiltonian, called dressed state, are a linear coupling of the bare cavity and TLS states, $|e\rangle\,|n\rangle$ and $|g\rangle\,|n+1\rangle$,

$$|+\rangle = \cos(\theta/2)\,|e,n\rangle + \sin(\theta/2)\,|g,n+1\rangle \tag{1.18}$$

$$|-\rangle = \sin(\theta/2)\,|e,n\rangle - \cos(\theta/2)\,|g,n+1\rangle\,, \tag{1.19}$$

where $\tan(\theta) = 2g\sqrt{n+1}/\Delta$, and eigenvalues

$$E_{\pm} = \pm\sqrt{\left(\frac{\Delta}{2}\right)^2 + g^2(n+1)}. \tag{1.20}$$

A general state evolving under the Jaynes–Cummings Hamiltonian [30] is

$$|\phi(t)\rangle\rangle = \sum_{n=0}^{\infty} c_n \left[a_+(n,t)|e,n\rangle + a_-(n,t)|g,n+1\rangle\right], \tag{1.21}$$

where c_n is initial photon distribution, and

$$a_+(n,t) = i\sqrt{n+1}\sin\left(\frac{g\sqrt{n+1}}{2}\right)\mathrm{e}^{i\Delta t/4}, \tag{1.22}$$

$$a_-(n,t) = \left[\cos\left(\frac{g\sqrt{n+1}t}{2}\right) - \frac{i\Delta}{2g}\sin\left(\frac{g\sqrt{n+1}t}{2}\right)\right]\mathrm{e}^{-i\Delta t/4}. \tag{1.23}$$

In the case of zero detuning ($\Delta = 0$), zero photons in the cavity, and a TLS in an initially excited state, we get what is known as the vacuum Rabi oscillations:

$$a_-(0,t) = \cos(gt/2)\,, \tag{1.24}$$
$$a_+(0,t) = i\sin(gt/2)\,. \tag{1.25}$$

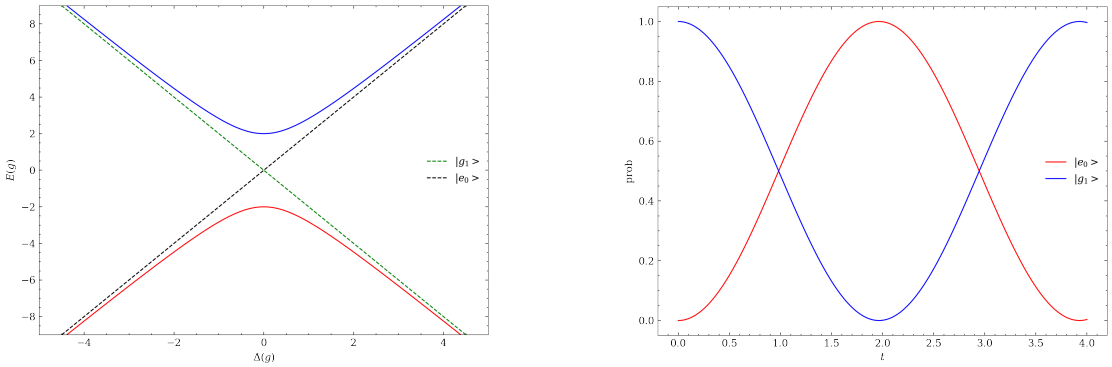

(a) Dressed states (b) Rabi oscillations

Figure 1.1: (a) The energies of the dressed states $|+\rangle$ (blue) and $|-\rangle$ (red). (b) Probability of the TLS being in the ground or excited state when resonant with cavity $\Delta = 0$. Highlighting the excitation swap with the cavity.

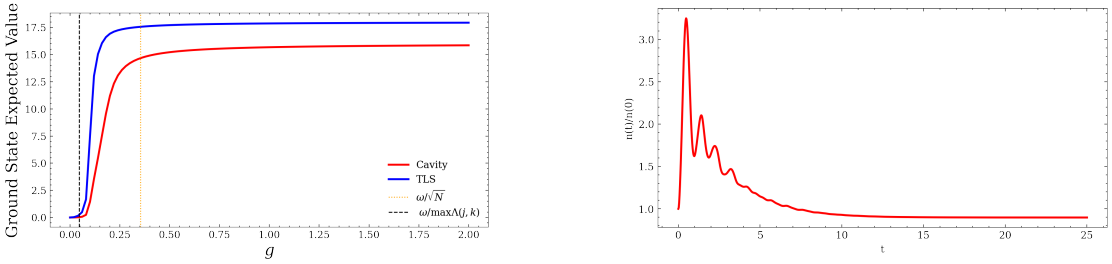

(a) Ground state occupation (b) Steady state solution

Figure 1.2: The JC model in the ultra–strong coupling regime, i.e. without the RWA approximation. (a) Ground state occupation of the cavity and TLS as the coupling strength is varied from the weak–coupling regime $g \ll 1$ to the ultra–strong coupling regime, $g \geq 1$. (b) Steady state solution of the cavity in the presence of photon loss, where $n(t) = \langle \hat{a}^\dagger \hat{a} \rangle_t$.

1.2 Extending to an Ensemble of Two–Level Systems

The Jaynes–Cummings model is the simplest model describing the interaction between a single TLS with a single cavity mode. However, as experimental techniques have progressed, interest in extending the Jaynes–Cummings model has increased. In this text we are interested in the extension of the Jaynes–Cummings model to an ensemble of identical TLS interacting with one cavity mode, known as the Tavis–Cummings model. The Tavis–Cummings system can be realized by an electron spin resonance system (ESR), where an ensemble of non–interacting electron spins in a large static magnetic field places inside high quality 3D cavity or coupled to 1D superconducting microwave cavities [42]. In ESR (and NMR) the ensembles are of the order of 10^3 to 10^{18} spins. However, unlike the Jaynes–Cummings model, the Tavis–Cummings model does not admit exact analytical solutions for arbitrary numbers of the TLS. As such, for a small number of spins, modelling the system becomes impossible. In chapter 2 we present a technique that allows us to determine the structure of the Tavis–Cummings model efficiently.

The Hamiltonian describing the Tavis–Cummings system [47] is

$$\hat{\mathcal{H}}_{\mathrm{TC}} = \omega_{\mathrm{tls}}\hat{J}_z + \omega_c\hat{a}^\dagger\hat{a} + g(\hat{J}_+\hat{a} + \hat{J}_-\hat{a}^\dagger), \tag{1.26}$$

where $\hat{J}_z$, $\hat{J}_x$ and $\hat{J}_\pm$ are collective spin operators. The collective spin operators are defined in terms of the single spin operators as such:

$$\hat{J}_z = \frac{1}{2}\sum_{i=1}^{N}\hat{\sigma}_z^{(i)},$$

$$\hat{J}_\pm = \sum_{i=1}^{N}\hat{\sigma}_\pm^{(i)},$$

where N is the number of two-level systems.

Similar to the JC Hamiltonian, the TC Hamiltonian [41, 47] conserves the total number of excitations, with excitation number operator

$$\hat{K} = \hat{a}^\dagger\hat{a} + \hat{J}_z, \tag{1.27}$$

and the interaction Hamiltonian can be analogously written in block–diagonal form. For the case $N = 2$, we have

$$\hat{\mathcal{H}}_{TC} = \begin{bmatrix} \Delta & \sqrt{n+1}g & \sqrt{n+1}g & 0 \\ \sqrt{n+1}g & 0 & 0 & \sqrt{n+2}g \\ \sqrt{n+1}g & 0 & 0 & \sqrt{n+2}g \\ 0 & \sqrt{n+2}g & \sqrt{n+2}g & -\Delta \end{bmatrix} \tag{1.28}$$

and is spanned by the four bare TLS–cavity states $\{|e\rangle|e\rangle|n\rangle, |e\rangle|g\rangle|n+1\rangle, |g\rangle|e\rangle|n+1\rangle, |g\rangle|g\rangle|n+2\rangle\}$.

The analogy with the JC model breaks down very quickly for general N. Fix the number of TLS, N, then the number of states for each excitation level k grows very fast

$$n(k) = \begin{cases} \sum_i^k \binom{N}{k} & k \leq N \\ 2^N & \text{otherwise} \end{cases}, \tag{1.29}$$

where $n(k)$ is the number of states at excitation level k. Thus, trying to directly diagonalize the system becomes very intractable very quickly for anything but very small k. Fortunately however, the TC model admits more symmetries than just the one given by total excitation, specifically the conservation of total angular momentum $\hat{J}^2 = \hat{J}_x^2 + \hat{J}_y^2 + \hat{J}_z^2$.

We will show in the next chapter how by leveraging the total angular momentum symmetry, we can reduce the problem into a more tractable one. In addition to total angular momentum symmetry, the TC model admits a continuous symmetry described by the circle group, U(1). The generator of the continuous symmetry has infinite eigenvalues, enumerated by $k \in N$, while the total angular momentum symmetry has eigenvalues $j = N/2, N/2-1, \ldots, 1/2(0)$ when N is even (odd). This additional symmetry is sufficient to make the TC model integrable and solvable, which is supported by the Bethe ansatz solution provided by Bogoliubov [6, 7, 8].

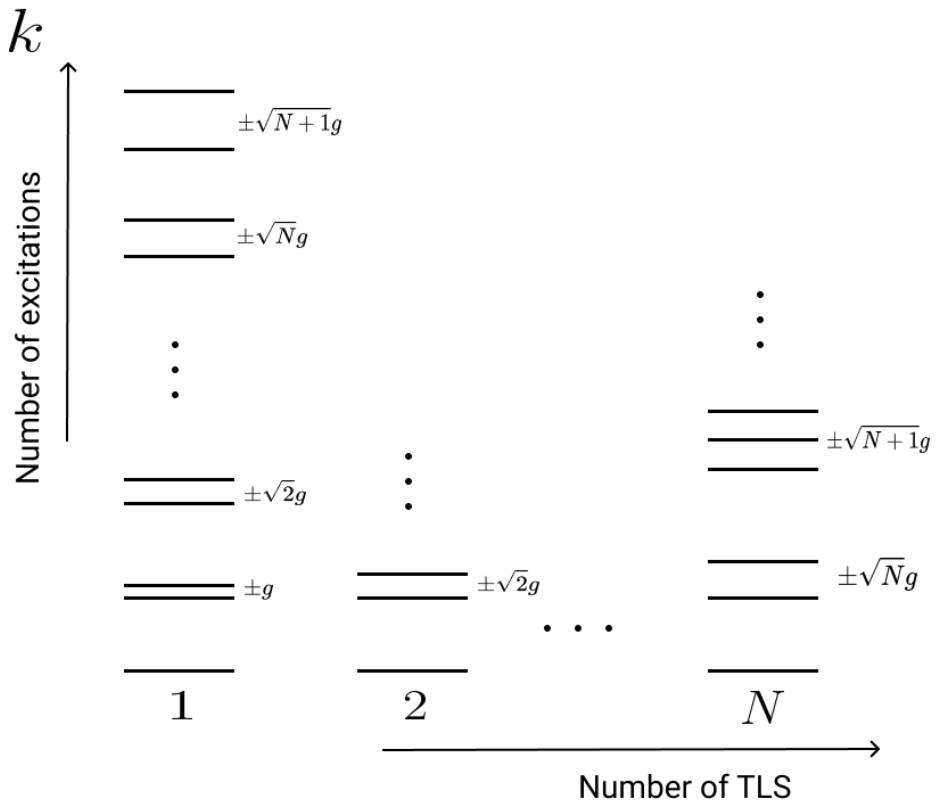

Figure 1.3: Structure of the energy spectrum of the TC Hamiltonian

1.2.1 Exact Analytical Solutions

In the next chapter we look closely at the structure of the TC Hamiltonian (1.26), however there are two of cases two cases in which exact analytical descriptions of the eigenstructure can be found. First, is the trivial case of zero TLS–cavity interaction. Second, is case where the Zeeman term is turned off. The latter of which is of interest in this text, and we describe here. Consider now the TC Hamiltonian prior to applying the RWA approximation

$$\hat{\mathcal{H}} = \omega_{\text{tls}}\hat{J}_z + \omega_c\hat{a}^\dagger\hat{a} + g(\hat{a}^\dagger + \hat{a})(\hat{J}_+ + \hat{J}_-), \tag{1.30}$$

This Hamiltonian admits a parity symmetry (symmetry group C_2), i.e. the Hamiltonian $\mathcal{H}$ commutes with the parity operator $\hat{\mathcal{P}} = e^{-i\pi(\hat{a}^\dagger\hat{a}+\hat{J}_z/2)}$. Now, we rotate the Hamiltonian

by $\pi/2$ around y. So we have

$$R_y(\pi/2) \ : \hat{J}_z \longmapsto \ \hat{J}_x = \hat{J}_+ + \hat{J}_- \tag{1.31}$$

$$\hat{J}_x \longmapsto \hat{J}_z, \tag{1.32}$$

and the Hamiltonian is

$$\hat{\mathcal{H}} = \omega_c \hat{a}^\dagger \hat{a} - \frac{\omega_{\text{tls}}}{2}(\hat{J}_+ + \hat{J}_-) + g(\hat{a}^\dagger + \hat{a})\hat{J}_z. \tag{1.33}$$

The Hilbert space of the TLS–cavity system is spanned by the basis $\{|\phi_n\rangle\,|j,m\rangle\}$, solving the model becomes that of finding what the $|\phi_n\rangle$ are. The idea is to use joint "coherent" states of the TLS and cavity . To that end, consider the displacement operator

$$\hat{a}' = \hat{a} + \frac{g}{\omega_c}\hat{J}_z, \tag{1.34}$$

the sum of the original annihilation operator of the cavity and $\hat{J}_z$. Then substituting (1.34) into (1.33), we get

$$\hat{\mathcal{H}} = \omega_c \left(\hat{a}'^\dagger \hat{a}' - \left(\frac{g}{\omega_c}\hat{J}_z \right)^2 \right) - \frac{\omega_{\text{tls}}}{2}(\hat{J}_+ + \hat{J}_-). \tag{1.35}$$

A quick calculation shows that $\hat{\mathcal{H}}$ commutes with $\hat{\mathcal{P}}$, so we did not lose the symmetries of the problem.

Before we solve for the coherent states of (1.34), we first find the action of $\hat{\mathcal{H}}$ on $|\phi_n\rangle\,|j,m\rangle$:

$$\begin{aligned}\hat{\mathcal{H}}\,|\phi_n\rangle\,|j,m\rangle = \omega_c \left(\hat{a}'^\dagger \hat{a}' - \left(\frac{gm}{\omega_c} \right)^2 \right) |\phi_n\rangle\,|j,m\rangle \\ - \frac{\omega_{\text{tls}}}{2}\,|\phi_n\rangle \left(\sqrt{j(j+1) - m(m+1))}\,|j,m+1\rangle + \sqrt{j(j+1) - m(m-1))}\,|j,m-1\rangle \right).\end{aligned} \tag{1.36}$$

We define coherent states of $\hat{a}'$ as we usually do as:

$$|\alpha\rangle = e^{-\frac{|\alpha|^2}{2}} \sum_{n=0}^{\infty} \frac{\alpha^n \hat{a}'^\dagger}{\sqrt{n!}}\,|0\rangle\,. \tag{1.37}$$

We can however simply substitute $\hat{J}_z$ in $\hat{a}'$ with the magnetization number m, such that we index the coherent states by m as follows:

$$\begin{aligned} |m\rangle &= e^{-\frac{|m|^2}{2}} \sum_{n=0}^{\infty} \frac{m^n \hat{a}'^{\dagger}}{\sqrt{n!}} |0\rangle \\ &= e^{-\frac{|m|^2}{2}} \sum_{n=0}^{\infty} \frac{m^n (\hat{a}^{\dagger} + \frac{g^2}{\omega_c^2} m^2)}{\sqrt{n!}} |0\rangle . \end{aligned} \tag{1.38}$$

Now if we go back to (1.36) and sub in the coherent states we defined above and take the limit as ω_{tls} goes to 0, we get the energies

$$E_{k,m} = \omega_c \left(k - \left(\frac{gm}{\omega_c} \right)^2 \right), \tag{1.39}$$

where k are the eigenvalues of the $(\hat{a}')^{\dagger}\hat{a}'$.

One of the features of this system is that ground state is degenerate with energies corresponding to $k = 0$ and $m = \pm N/2$ and eigenstates

$$|\pm\rangle = \frac{1}{\sqrt{2}}(|-N/2\rangle\,|N/2, N/2\rangle \pm |N/2\rangle\,|N/2, -N/2\rangle), \tag{1.40}$$

which respects the parity symmetry of our Hamiltonian. Another interesting feature of the ground states of this system, is the mean number of photons in the cavity is $N/2$, which will be quite large for the ensemble of TLS we are interested in. So the non–RWA–TC model is analytically solvable in the limit of zero–Zeeman term.

Chapter 2

Structure of the Tavis–Cummings Model

Consider a TLS–cavity system with no interaction term, that is set the coupling strength to $g = 0$ in (1.26), we can then observe a few properties. First, the ground state of the TLS ensemble is the state where all the TLS are in their ground state $|N/2, -N/2\rangle$. Second, the number of states is $\sum_{j=0}^{N/2} 2j + 1 = N^2$ not the full 2^N space of possible states. This gap is due to the degeneracy of each subspace. One can easily find the degeneracy of each subspace labeled by the total angular momentum of the TLS

$$d_j = \frac{(2j+1)N!}{(N/2+j+1)!(N/2-j)!}, \tag{2.1}$$

for $j = N/2, N/2-1, \ldots$, and we do indeed recover the full space of states

$$\sum_{j=0}^{N/2}(2j+1)d_j = \sum_{j=0}^{N/2}\frac{(2j+1)^2 N!}{(N/2+j+1)!(N/2-j)!} \tag{2.2}$$

$$= 2^N. \tag{2.3}$$

Thus, we notice that if we enumerate our states with the total angular momentum j — which is conserved— we can reduce the dimensionality of our problem from 2^N to N^2. Now, going back to the interacting TC model, we will define a new basis in which to diagonalize the Hamiltonian (1.26) labeled by total angular momentum j and excitation number k. For a fixed value of k, the total number of states in each subspace is

$$n_k(j) = \min(k+1, 2j+1), \tag{2.4}$$

and basis states

$$\mathcal{B}_{j,k} = \{|k - i - j - N/2\rangle\,|j, i - j\rangle \;\mid k \in \{1, n_k(j) + 1\}\}. \tag{2.5}$$

This basis can be understood in this way; in the k'th excitation level and the subspace with total angular momentum j, the basis is the set of all states enumerating the TLS and the cavity excitation exchanges up to $n_k(j) = \min(k + 1, 2j + 1)$. This simple basis change is enough to allow us to extract statistical descriptions and to efficiently numerical simulate dynamics of the TC model. Figure 2.1 illustrates the effect of this basis change on the eigenstructure of the TC Hamiltonian.

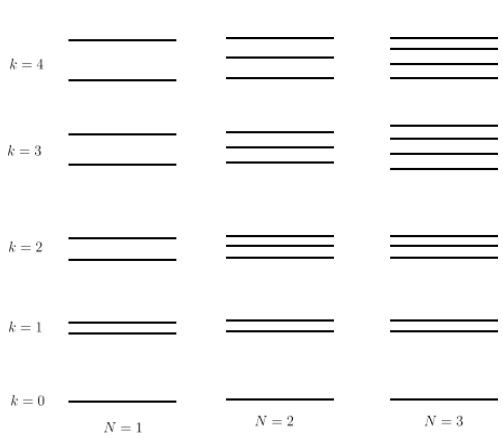

(a) Basis enumerated by excitation level k

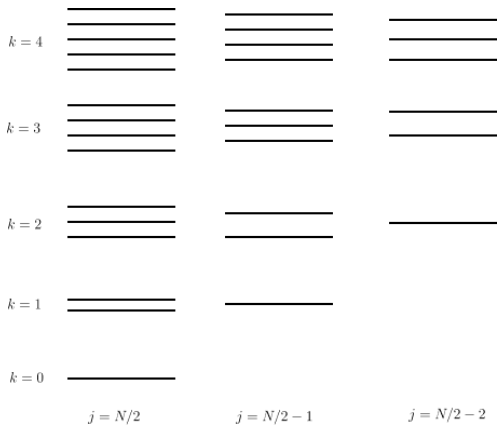

(b) Basis enumerated by excitation level k and total angular momentum j

Figure 2.1: Energy diagrams of the TC model Hamiltonian in the basis of bare states of the TLS-cavity on resonance ($\Delta = 0$) (a) and in the basis of $\mathcal{B}_{j,k}$ of the two quantum numbers k and j (b).

2.1 Diagonalization

Consider the resonant case, such that $\omega_{\text{tlc}} = \omega_c = \omega$. Then TC Hamiltonian (1.26) in the $\mathcal{B}_{j,k}$ basis can be written in the following way:

$$\hat{\mathcal{H}}_{TC} = \bigoplus \left(\omega k + gL(j,k)\right), \tag{2.6}$$

where $L(j,k)$ is the coupling matrix, describing the interaction between the states in the j angular momentum subspace and k'th excitation level. Looking at figure 2.1b one sees that the only transitions allowed by the interaction Hamiltonian is a single excitation transfer left $(j+1)$ or right $(j-1)$ in each excitation level k. Thus, the coupling matrix takes the form a symmetric tridiagonal matrix with zero diagonal:

$$L(j,k) = \begin{bmatrix} 0 & l_1(j,k) & & & \\ l_1(j,k) & 0 & l_2(j,k) & & \\ & l_2(j,k) & 0 & \ddots & \\ & & \ddots & \ddots & l_n(j,k) \\ & & & l_n(j,k) & 0 \end{bmatrix}, \tag{2.7}$$

where the matrix elements $l_i(j,k)$ are given by

$$\begin{aligned} l_i(j,k) &= \langle k-i-j-N/2| \langle j, i-j| \hat{\mathcal{H}}_{int} |k-i-j-N/2-1\rangle |j, i-j+1\rangle & (2.8)\\ &= \sqrt{(2ij - i(i-1))\,(k - n_k(j) - i + 1)}. & (2.9) \end{aligned}$$

Hence, diagonalizing the coupling matrices (2.7) would provide us with a full description of the eigenstuructre of the TC Hamiltonian (1.26). Unfortunately there is no general analytic solutions to these class of matrices, also known as Jacobi operators. However, there exists efficient numerical methods [15] for calculating the eigenvalues of symmetric tridiagonal matrices in $\mathrm{O}(n \log n)$ time and eigenvectors in $\mathrm{O}(n^2)$ time, where in the case of our operators of interest we have $n = n_k(j)$. While analytical solutions might not exist, by switching to the $\mathcal{B}_{j,k}$ basis we can efficiently calculate the eigenenergies and eigenstates for each subspace of interest for large excitation levels k and TLS N.

Nevertheless, we can still gain some insight into the structure of the TC model without relying on any numerical methods. For example, one can easily see that the spectrum of the coupling matrix is symmetric. That is for each eigenvalue λ in the spectrum of $L(j,k)$, $-\lambda$ is also an eigenvalue of $L(j,k)$ [51]. Other insights can be found as we will show in the next section.

2.2 Statistics of The Coupling Matrix

In this section we describe some statistics of the eigenvalues of the coupling matrix $L(j,k)$. Diagonalizing the coupling matrix in the $\mathcal{B}_{j,k}$ basis allows us to easily bound maximal eigenvalue and find the angular momentum subspaces for which the dynamics of the system are most relevant. This in turns aids in efficiently simulating the dynamics of the TC model and calculate important values for experimental set ups.

2.2.1 Maximally Degenerate Subspace

A common approximation of the TC model is to consider only the maximally symmetric subspace, also known as the Dicke subspace. The Dicke subspace approximation well approximates the dynamics of the TC system in certain regimes, low temperatures and dynamics near the ground state. However, this single subspace approximation fails for warmer systems. One then wonders if there is a subspace or a collections of subspaces that well approximates the dynamics of the system. A natural consideration is the most degenerate subspace, which we will denote j^*.

We have from (2.1) that the degeneracy d_j of each angular momentum subspace j is given by

$$d_j = \frac{(2j+1)N!}{(N/2+j+1)!(N/2-j)!}. \tag{2.10}$$

We take the continuous extension of the binomial function:

$$\binom{N}{k} = \frac{\Gamma(N+1)}{\Gamma(k)\Gamma(N-k+1)}, \tag{2.11}$$

such that (2.10) can be written as a continuous function in j

$$d_j = \frac{2j+1}{N/2+j+1}\frac{\Gamma(N+1)}{\Gamma(N/2+j+1)\Gamma(N/2-j+1)}. \tag{2.12}$$

To find the maximum we first find

$$\frac{d}{dj}d_j = 4\binom{N}{N/2+j}\frac{\frac{1}{2}(2j+1)(N+2j+2)(H_{N/2-j}-H_{N/2+j})+N+1}{(N+2j+2)^2}, \tag{2.13}$$

where H_k is the Harmonic series. The degeneracy is then maximal when

$$\frac{1}{2}(2j+1)(N+2j+2)(H_{N/2-j}-H_{N/2+j})+N+1=0. \tag{2.14}$$

Using the identity $H_x = \log x + \gamma + \mathrm{O}(x^{-1})$, where γ is the Euler–Mascheroni constant and simplifying, we are left with

$$\frac{1}{2}(2j+1)(N+2j+2)\log\left(\frac{N/2-j}{N/2+j}\right) + N + 1 = 0. \tag{2.15}$$

Then for $j^* = \frac{\sqrt{N}-1}{2} + \frac{1}{6\sqrt{N}}$ and $N \gg 1$, we reduce to

$$\frac{1}{\sqrt{N}} + \mathrm{O}\left(\frac{1}{N}\right), \tag{2.16}$$

Thus, we have that the maximally degenerate angular momentum subspace is

$$j^* = \mathrm{O}\left(\sqrt{N}\right). \tag{2.17}$$

This means that as the number of spins N increases, the most degenerate subspace j^* is increasingly separated from the Dicke subspace.

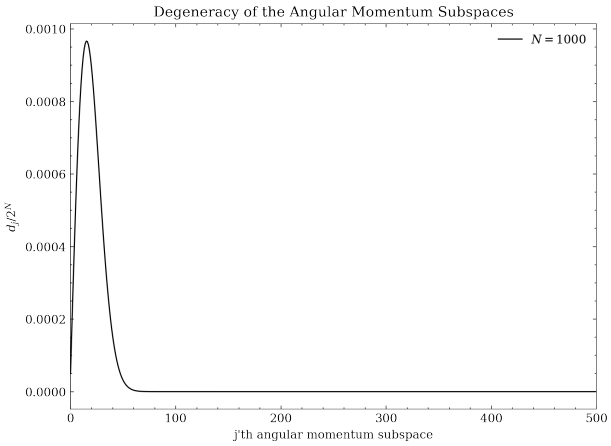

Figure 2.2: Plot of the angular momentum subspace j vs the it's scaled degeneracy $d_j/2^N$ for $N = 1000$ showing a peak at $j = 15$.

As can be seen in figure 2.2, the essential support of is approximately given by $j \in 0, 1, \ldots, 2\sqrt{N}$. That is most of the states in the system are contained within the first $2\sqrt{N}$ angular momentum subspaces. This means that for simulating the dynamics of very large systems that would otherwise be very computationally demanding, one can instead restrict themselves to the first $2\sqrt{N}$ angular momentum subspaces, gaining a quadratic speed up. This speed up means that the original reduction from 2^N to $\mathrm{O}(N^2)$ states can be further reduced to $\mathrm{O}(N)$. This analysis also holds for any quantum system whose total angular momentum is a constant of motion.

2.2.2 Maximal Energy

An important aspect of the TC model is the energy range we need to consider in our experimental design. We can find an upper bound on the energy range by bounding the largest eigenvalue of the coupling matrix (2.7) for each j and k. Let $\Lambda(j,k)$ denote the spectrum of the coupling matrix $L(j,k)$, then we wish to find an upper bound on the largest eigenvalue $\max \Lambda(j,k)$. To this end, consider the tridiagonal Toelpitz matrix

$$A_n = \begin{bmatrix} a & b & 0 & 0 & \cdots & 0 \\ c & a & b & 0 & \cdots & 0 \\ 0 & c & a & b & \cdots & 0 \\ \vdots & \vdots & \vdots & \ddots & \cdots & 0 \\ \vdots & \vdots & \vdots & \vdots & a & b \\ 0 & 0 & 0 & \cdots & c & a \end{bmatrix}, \tag{2.18}$$

with eigenvalues given by [37]

$$\lambda_k = a + 2\sqrt{bc}\cos\frac{k\pi}{n+1}, \tag{2.19}$$

for $k = 1, 2, \ldots, n$. Now consider the case of a symmetric tridiagonal but not Toelpitz matrix

$$B_n = \begin{bmatrix} 0 & b_1 & 0 & 0 & \cdots & 0 \\ b_1 & 0 & b_2 & 0 & \cdots & 0 \\ 0 & b_2 & 0 & b_3 & \cdots & 0 \\ \vdots & \vdots & \vdots & \ddots & \cdots & 0 \\ \vdots & \vdots & \vdots & \vdots & 0 & b_{n-1} \\ 0 & 0 & 0 & \cdots & b_{n-1} & 0 \end{bmatrix}, \tag{2.20}$$

with all entries non–negative and each b_i bounded above such that $b_i \leq b_{\max}$ for all i. Then the eigenvector with the largest eigenvalue's entries must all be positive and it's eigenvalue is monotonically increasing in b_i. In the Toelpitz case, the largest eigenvalue is $2b\cos\frac{1}{n+1}$. Thus, in the symmetric tridiagonal case the supremum of the eigenvalues is $2b_{\max}\cos\frac{1}{n+1}$.

Going back to our coupling matrix, we have that each $l_i(j,k)$ is non–negative and bounded by $j\sqrt{k}$, and $n_{j,k} = \min\{2j+1, k+1\}$. Thus, the supremum of the eigenvalues of the coupling matrix $L(j,k)$ is

$$\sup\Lambda(j,k) = \begin{cases} 2j\sqrt{k}\cos\frac{1}{2(2j+1)}, & n_j(k) = 2j+1 \\ 2j\sqrt{k}\cos\frac{1}{2}, & n_j(k) = k+1 \end{cases}. \tag{2.21}$$

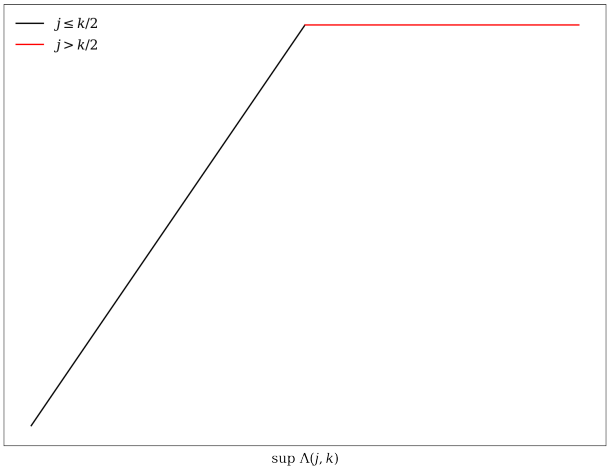

Figure 2.3: Plot of the upper bound of the eigenenergies of $L(j,k)$ for fixed excitation level k.

Bounding the maximal energy can be used to set a tighter bound on g, for which the RWA approximation is valid. The standard criterion for the strong–coupling regime of an ensemble of TLS is [32]

$$g\sqrt{N} \ll \omega. \tag{2.22}$$

As we can see in figure 2.4, this does not provide an adequate description of the validity of the rotating wave approximation. Instead, equipped with the means of calculating the maximal energy of each subspace of the coupling matrix, we then naturally set a tighter criterion of

$$g \max \Lambda(j,k) \ll \omega. \tag{2.23}$$

This puts a limit on j and k, for which the RWA holds.

2.3 Semi–Classical Approximation of Density of States

A tractable way to describe features of the TC model for a large number of spins is by restricting ourselves to the fully symmetric subspace (Dicke subspace) and using a semi–classical approach, by which we can produce analytic results for the thermal behaviour of the spin–cavity system. We are mainly interested in the thermal dynamics of the TC

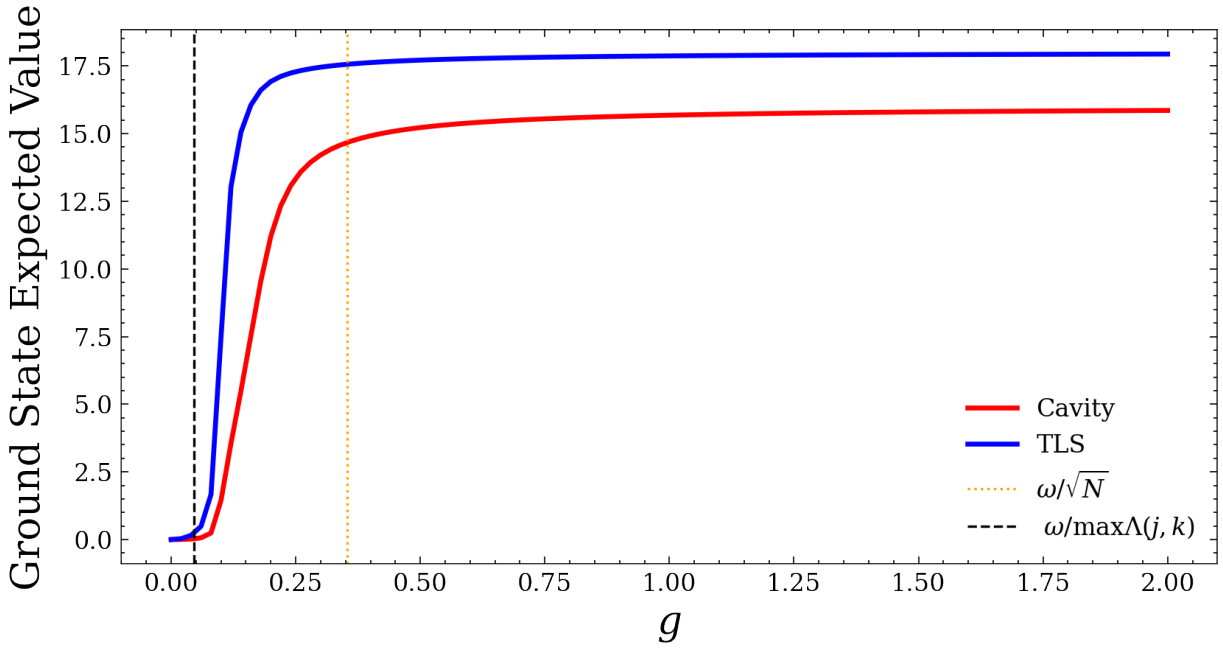

Figure 2.4: Plot of the ground state occupation vs the coupling strength g. In the ultra–strong coupling regime, the ground state has both photonic (red) and TLS excitations (blue). The transition from the strong to the ultra–strong coupling regime is not adequately captured by standard criterion of $g \ll \omega/\sqrt{N}$. Meanwhile our criterion of $g \ll \omega/\max\Lambda(j,k)$ captures this transition very accurately.

model by way of computing the partition function. Since the partition function is simply the Laplace transform of the density of states, we need only concern ourselves with calculating the density of states. The resonant TC Hamiltonian is once again

$$\hat{\mathcal{H}} = \omega \hat{a}^\dagger \hat{a} + \omega \hat{J}_z + g(\hat{a}\hat{J}_+ + \hat{a}^\dagger \hat{J}_-). \tag{2.24}$$

The semi–classical density of states of the TC model in the Dicke subspace well approximates the fully quantum density of states in the thermodynamic limit. The semi–classical Hamiltonian is given by substituting the spin operators $\hat{J}_i$ with classical angular momentum variables j_i and substituting the cavity operators with classical harmonic variables q and p [5, 18]. The semi–classical Hamiltonian is then

$$\hat{\mathcal{H}} = \frac{\omega}{2}(q^2 + p^2) + \omega j_z + g\sqrt{j}\sqrt{1 - \frac{j_z^2}{j^2}}\left[q\cos\phi - p\sin\phi\right], \tag{2.25}$$

where $\phi = \arctan(j_y/j_x)$.

The density of states equation is given by [26]

$$\nu(E) = \frac{1}{(2\pi)^2}\int \mathrm{d}q\ \mathrm{d}p\ \mathrm{d}\phi\ \mathrm{d}j_z\ \delta\left(E - \mathcal{H}\left(q, p, \phi, j_z\right)\right), \tag{2.26}$$

which we now need to evaluate. Recall the identity $\delta(g(x)) = \sum_i \frac{\delta(x-x_i)}{|g'(x_i)|}$, where x_i are the real roots of $g(x)$. We first integrate over q, so we can rewrite $\delta\left(E - \mathcal{H}\left(q, p, \phi, j_z\right)\right) = \frac{\delta(q-q_+)}{|\partial\mathcal{H}/\partial q|_{q_+}} + \frac{\delta(q-q_-)}{|\partial\mathcal{H}/\partial q|_{q_-}}$, where q_+ and q_- are the real roots of the quadratic equation $E - \mathcal{H}\left(q, p, \phi, j_z\right)$, such that

$$\nu(E) = \frac{1}{(2\pi)^2}\int \mathrm{d}j_z\ \mathrm{d}\phi\ \mathrm{d}p\ \mathrm{d}q\ \left(\frac{\delta\left(q - q_+\right)}{|\partial\mathcal{H}/\partial q|_{q_+}} + \frac{\delta\left(q - q_-\right)}{|\partial\mathcal{H}/\partial q|_{q_-}}\right). \tag{2.27}$$

The roots are

$$\omega q_\pm = -g\sqrt{j}\cos\phi\sqrt{\left(1 - \frac{j_z^2}{j^2}\right)} \pm \sqrt{-\omega^2 p^2 + bp + c}, \tag{2.28}$$

where

$$b = 2\omega g\sqrt{j}\sin\phi\sqrt{\left(1 - \frac{j_z^2}{j^2}\right)}, \tag{2.29}$$

$$c = g^2 j\cos\phi^2\left(1 - \frac{j_z^2}{j^2}\right) + 2\omega(E - \omega j_z). \tag{2.30}$$

In addition, we have

$$|\partial\mathcal{H}/\partial q|_{q_+} = |\partial\mathcal{H}/\partial q|_{q_-} = \sqrt{-\omega^2 p^2 + bp + c}. \tag{2.31}$$

We then integrate with respect to q from q_- to q_+ and obtain simply

$$\nu(E) = \frac{1}{(2\pi)^2} \int \mathrm{d}j_z \; \mathrm{d}\phi \; \mathrm{d}p \; \frac{2}{\sqrt{-\omega^2 p^2 + bp + c}}. \tag{2.32}$$

Next, we repeat the procedure once more for p. The limits of the integration must be such that denominator has real roots in p, so we must have

$$b^2 - 4\omega^2 c \geq 0. \tag{2.33}$$

But first, we can rewrite the integral as

$$\nu(E) = \frac{1}{(2\pi)^2} \int \mathrm{d}j_z \; \mathrm{d}\phi \; \mathrm{d}p \; \frac{1}{\sqrt{-\omega^2 (p - p_+)(p - p_-)}}, \tag{2.34}$$

and integrate from p_- to p_+ and obtain

$$\nu(E) = \frac{1}{\omega(2\pi)^2} \int \mathrm{d}j_z \; \mathrm{d}\phi. \tag{2.35}$$

The roots $p_\pm$ are real when

$$\frac{jg^2}{2\omega} - \frac{j_z^2 g^2}{j\omega} - \omega j \geq -E, \tag{2.36}$$

which leaves us with three cases in E. First, when $E_{\min} \leq E < -\omega j$, we have that $j_z \in [a_-, a_+]$ holds, where

$$a_\pm = \frac{jg^2}{2\omega} \pm \frac{g}{\omega}\sqrt{2(E - E_{\min})}. \tag{2.37}$$

Second case is for $-\omega j < E < \omega j$, we have $j_z \in [-\omega j, a_+]$. Finally, for $E > \omega j$ we have $j_z \in [-\omega j, \omega j]$. In addition, we have no restrictions on ϕ, so $\phi \in [0, 2\pi)$. Integrating with respect to j_z and ϕ we obtain

$$\nu(E) = \begin{cases} \dfrac{2jg}{\omega^2}\sqrt{2(E - E_{\min})}, & E_{\min} \leq E < -\omega j \\ \dfrac{j}{\omega}\left[1 - \omega^2/g^2 + \omega/g\sqrt{2(E - E_{\min})}\right], & -\omega j < E < \omega j \\ \dfrac{2j}{\omega}, & E > \omega j \end{cases}. \tag{2.38}$$

This technique can be extended to the rest of the angular momentum subspaces, since in the TC model each angular momentum sector is decoupled from the rest in the block diagonal basis $\beta_{j,k}$. Thus we can write the semi–classical density of states for all the angular momentum sectors as

$$\nu(E) = \sum_{j=0}^{N/2} d_j \nu(E, j). \tag{2.39}$$

However, the semi–classical approximation is only good for large N and low temperatures, so that the approximation begins to break down for small j. If the state of the system is populated by states in the lowest lying angular momentum sectors then the approximation will fail. This may not be of concern in the thermodynamic limit $N \longrightarrow \infty$. However, for finite N and general dynamics, the semi–classical approximation will not suffice.

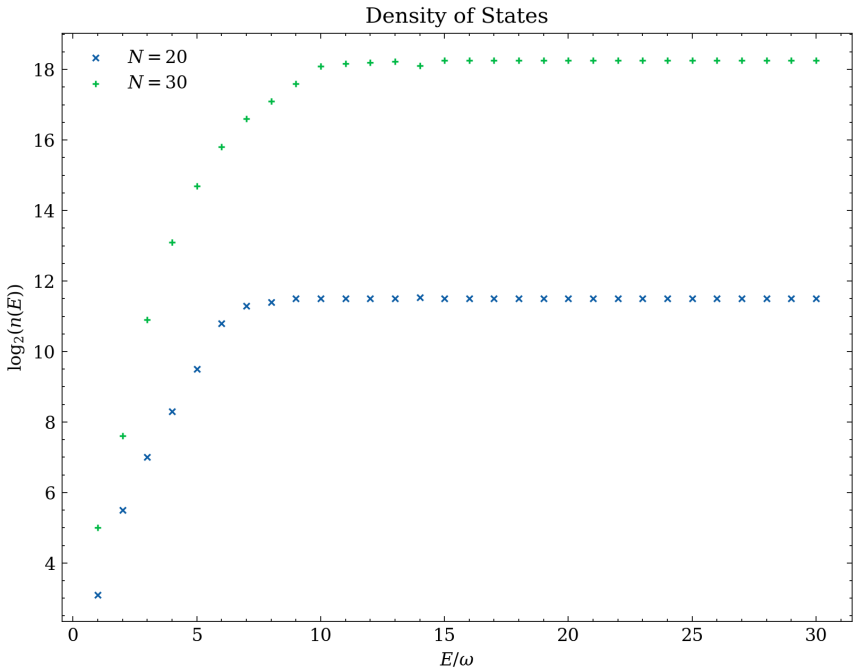

Figure 2.5: Numerical results for the scaled density of states of the TC Hamiltonian, for $\omega/g = 100$.

Chapter 3

Dynamics of the Tavis–Cummings Model

In this chapter we examine some dynamics of the Tavis–Cummings model. We begin by solving for the steady state solution of TC model with and without the RWA in the presence of dissipation, which provides a better understanding of the symmetries of the TC model. Next, we show that by modulating the TLS–cavity coupling strength g, we can achieve close to full population transfer from the ground to the excited states the TLS and vice–versa. Finally, we briefly discuss entanglement and notion of quantum "collectiveness" as pertain to light–matter interaction, and propose a measure for quantum collectiveness.

3.1 Steady State Solutions in The Presence of Photon Loss

The full TC model (Dicke model) without the RWA approximation

$$\hat{\mathcal{H}}_{\text{Dicke}} = \omega_{\text{tls}}\hat{J}_z + \omega_c\hat{a}^\dagger\hat{a} + g(\hat{a}^\dagger + \hat{a})(\hat{J}_+ + \hat{J}_-) \tag{3.1}$$

is markedly different different than the one with the RWA approximation

$$\hat{\mathcal{H}}_{\text{TC}} = \omega_{\text{tls}}\hat{J}_z + \omega_c\hat{a}^\dagger\hat{a} + g(\hat{J}_+\hat{a} + \hat{J}_-\hat{a}^\dagger). \tag{3.2}$$

Mainly, the discrete parity symmetry that the Dicke Hamiltonian admits turns into a continuous one U(1) symmetry. This means that the TC model is integrable (exactly

solvable), unlike the Dicke model [6, 7]. This in turn however, means that the Dicke Hamiltonian's structure and dynamics are different than that of the TC Hamiltonian. One way in which the dynamics differ is in the steady state solutions in the presence of photon loss. The Markovian master equation [11] describing the non–unitary time evolution of the density matrix $\hat{\rho}$ of the TLS–cavity system with photon dissipation rate κ is

$$\partial_t \hat{\rho} = -i\Big[\hat{\mathcal{H}}, \hat{\rho}\Big] + \kappa(2\hat{a}\hat{\rho}\hat{a}^\dagger - \hat{a}^\dagger\hat{a}\hat{\rho} - \hat{\rho}\hat{a}^\dagger\hat{a}), \tag{3.3}$$

for $\hat{\mathcal{H}} = \hat{\mathcal{H}}_{\text{Dicke}},\ \hat{\mathcal{H}}_{\text{TC}}$. For which the time evolution of the expectation for an arbitrary operator $\hat{A}$ is

$$\partial_t \langle \hat{A} \rangle = i\langle \Big[\hat{A}, \hat{\mathcal{H}}\Big] \rangle + \kappa\langle 2\hat{a}\hat{A}\hat{a}^\dagger - \hat{a}^\dagger\hat{a}\hat{A} - \hat{A}\hat{a}^\dagger\hat{a} \rangle. \tag{3.4}$$

In our case we are interested in expectation of the photon number $\hat{A} = \hat{a}^\dagger\hat{a}$,

$$\partial_t \langle \hat{a}^\dagger\hat{a} \rangle = i\langle \Big[\hat{a}^\dagger\hat{a}, \hat{\mathcal{H}}\Big] \rangle + 2\kappa\langle (\hat{a}\hat{a}^\dagger)^2 - (\hat{a}^\dagger\hat{a})^2 \rangle. \tag{3.5}$$

We can see in figure 3.1 that in the presence of photon losses the TC model decays exponentially, with rate approximately given by $1/\kappa$, to the state with zero photons and TLS in their ground states. Furthermore, one can verify that the total excitation $\hat{K}$ symmetry is not broken in presence of photon losses. Indeed we have that the master equation is invariant under the following unitary rotations of the Hamiltonian and the photon loss Lindblad operator $\hat{a}$

$$\hat{\mathcal{H}}_{\text{TC}} \longrightarrow e^{i\hat{K}\theta}\hat{\mathcal{H}}_{\text{TC}}e^{-i\hat{K}\theta}, \tag{3.6}$$

$$\hat{a} \longrightarrow e^{i\hat{K}\theta}\hat{a}e^{-i\hat{K}\theta}. \tag{3.7}$$

This should mean that excitation should be conserved, but for Lindblad master equations, symmetry does not imply that the corresponding quantity is conserved [2]. That is if the initial state is in the k'th excitation subspace in the presence of photon losses, then it will not stay there but indeed move down the excitation ladder at an exponential rate.

In contrast, the Dicke model reaches a non–trivial steady state with some number of photons still in the cavity. The reason is that unlike the continuous symmetry in the TC model allowing us to decompose the interaction Hamiltonian into block diagonals of $\hat{K}$ sectors. The Dicke Hamiltonian allows transitions up and down the excitation ladder, since $\hat{K}$ is not conserved, as can be seen from the non–zero elements in figure 3.2. So while in TC model photon losses allows for the decay into fewer excitation sectors, with no path upwards. The Dicke Hamiltonian allows for excitation increase and decrease, and the steady state is the balancing of both processes.

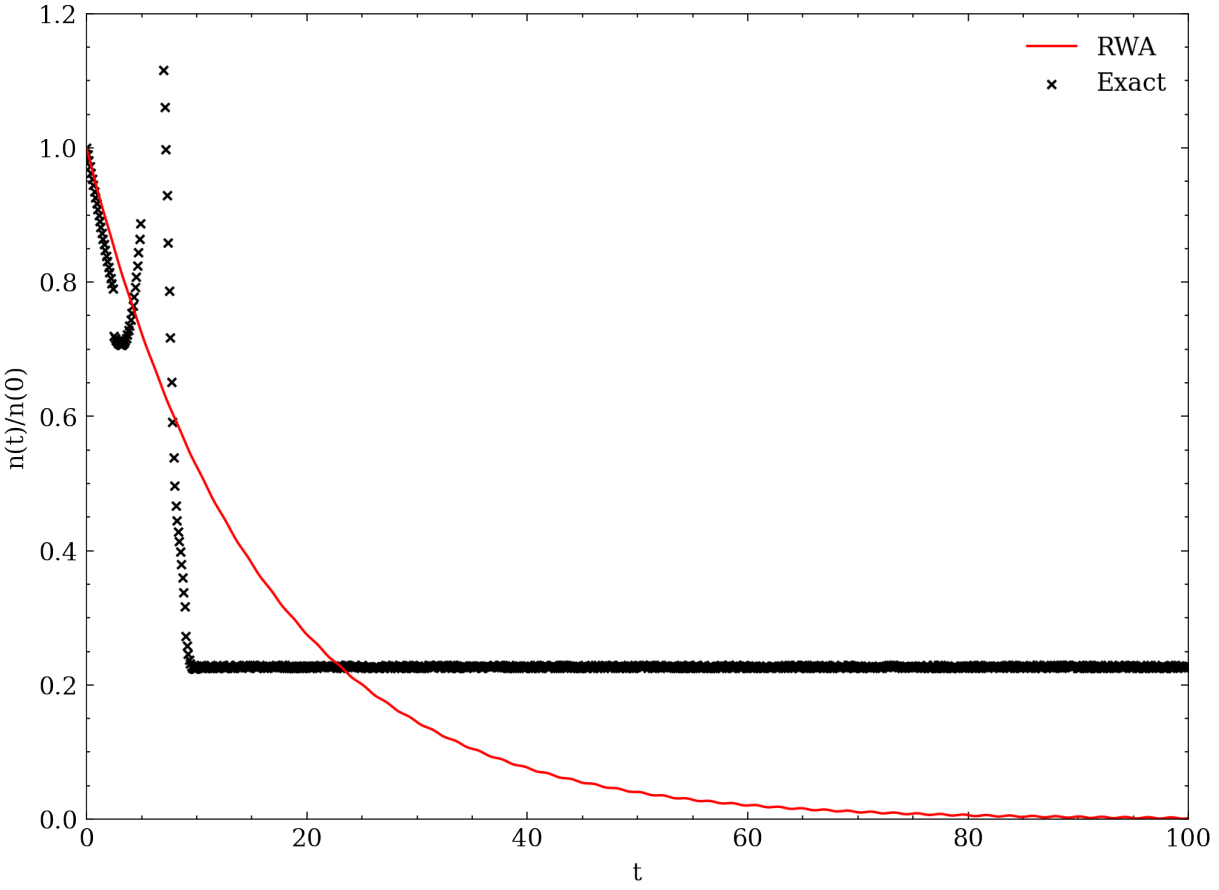

Figure 3.1: Time evolution of the photon number in the cavity for the TLS–cavity model with and without the RWA approximation in the presence of photon loss, for $N = 30$.

3.2 Phase Modulation of The Coupling Strength

In this section we explore how modulating the TLS–cavity strength g can affect the dynamics of an ensemble of TLS sufficiently detuned from the cavity. Specifically, starting with an ensemble of TLS in their excited states, we drive TLS to their ground states by modulating the TLS–cavity coupling strength g. The Hamiltonian describing such a system has the form

$$\hat{\mathcal{H}} = \omega_c \hat{a}^\dagger \hat{a} + \omega_{\text{tls}} \hat{J}_z + g(f(t)\hat{J}_+ \hat{a} + f(t)^* \hat{J}_- \hat{a}^\dagger). \tag{3.8}$$

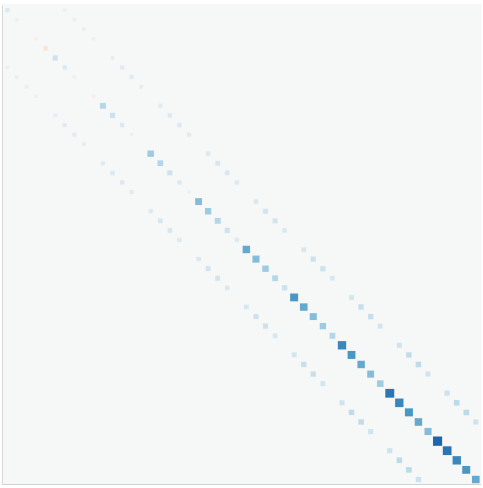

Figure 3.2: Structure of the Dicke Hamiltonian, $N = 4$ and k up to 16.

We focus on the simple of case of sinusodial modulation

$$\hat{\mathcal{H}} = \omega_c \hat{a}^\dagger \hat{a} + \omega_{\text{tls}} \hat{J}_z + \frac{g}{2}(\sin(\omega_{\text{drive}} t) + 1)(\hat{J}_+ \hat{a} + \hat{J}_- \hat{a}^\dagger). \tag{3.9}$$

The interaction part of the Hamiltonian is responsible for the excitation transfers between the TLS ensemble and the cavity and TLS–TLS interactions mediated by the cavity. However, when the TLS and cavities are detuned, i.e. $|\omega_c - \omega_{\text{tls}}| \gg g$, population transfer is highly suppressed. It is easy to see that the appropriate choice of the driving frequency is $\omega_{\text{drive}} = |\omega_c - \omega_{\text{tls}}|$. To see why this is true, we restrict ourselves to the case of a single TLS and proceed with routine time–dependent perturbation theory. The interaction Hamiltonian in the Dirac picture is given by

$$\begin{aligned} \hat{\mathcal{H}}^D_{\text{int}} &= e^{-i(\omega_c \hat{a}^\dagger \hat{a} + \omega_{\text{tls}} \hat{J}_z)t} \hat{\mathcal{H}}_{\text{int}} e^{i(\omega_c \hat{a}^\dagger \hat{a} + \omega_{\text{tls}} \hat{J}_z)t} \\ &= \frac{g}{2}(\sin(\omega_{\text{drive}} t) + 1)(\hat{J}_+ \hat{a} e^{i\Delta\omega t} + \hat{J}_- \hat{a}^\dagger e^{-i\Delta\omega t}), \end{aligned} \tag{3.10}$$

where $\Delta\omega = |\omega_c - \omega_{\text{tls}}|$ is the TLS–cavity detuning.

The transition probability to first order from excited to ground state is given by

$$P_{1\to 0} = \lambda^2 \left| \frac{g}{2} \int_0^t dt_1 \ (\sin(\omega_{\text{drive}}\ t_1) + 1) \left(\mathcal{V}_{10} e^{i\Delta\omega t} + \mathcal{V}_{10}^\dagger e^{-i\Delta\omega t} \right) \right|^2, \tag{3.11}$$

where λ is the pertubative parameter and

$$\mathcal{V}_{10} = \langle 0| \hat{J}_+ |1\rangle , \tag{3.12}$$

$$\mathcal{V}_{10}^\dagger = \langle 0| \hat{J}_- |1\rangle . \tag{3.13}$$

Evaluating the integral we get

$$P_{1\to 0} = \frac{\lambda^2 g^2}{4} \left| \frac{(A+B)}{(\Delta\omega - \omega_{\text{drive}})(\Delta\omega + \omega_{\text{drive}})} - \frac{C}{\Delta\omega} \right|^2 , \tag{3.14}$$

where

$$A = \omega_{\text{drive}}((\mathcal{V}^\dagger)_{10} - \mathcal{V}_{10})e^{it\Delta\omega} + \omega_{\text{drive}} \cos(\omega_{\text{drive}}\ t)(\mathcal{V}_{10} + \mathcal{V}_{10}^\dagger e^{2it\Delta\omega}),$$

$$B = i\Delta\omega \sin(\omega_{\text{drive}}\ t)(\mathcal{V}_{10} - \mathcal{V}_{10}^\dagger e^{2it\Delta\omega}),$$

$$C = i(e^{it\Delta\omega} - 1)(\mathcal{V}_{10} + \mathcal{V}_{10}^\dagger e^{it\Delta\omega}).$$

So, by choosing the driving frequency ω_{drive} to be close to the detuning frequency, i.e. $|\Delta\omega - \omega_{\text{drive}}| \ll \Delta\omega + \omega_{\text{drive}}$, we maximize the transition probability between the excited and ground state.

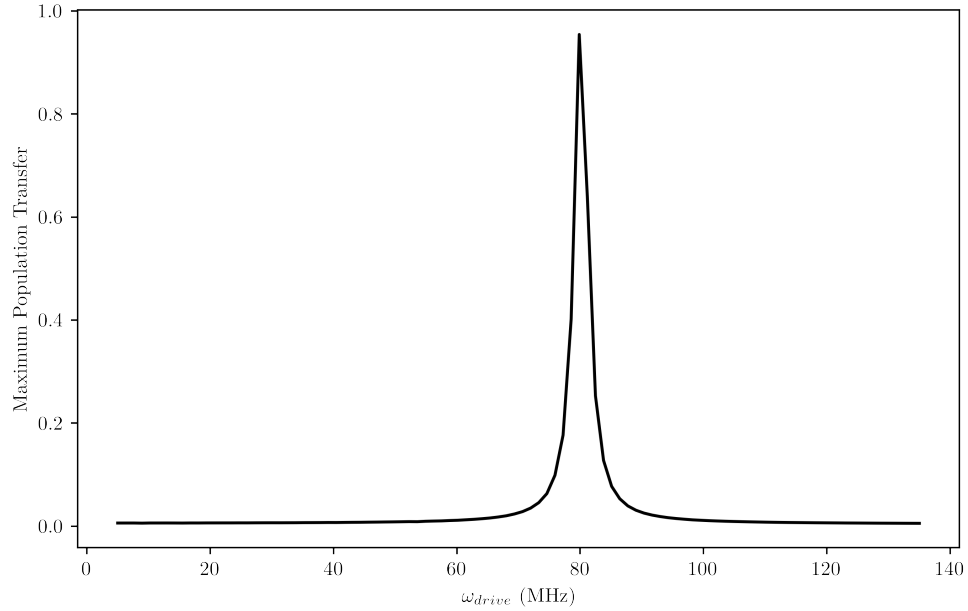

Figure 3.3: Numerical simulation of the maximum population transfer for each ω_{drive}, for $\omega_c = 3$ GHz and $\omega_{\text{tls}} = 3.08$ GHz for $N = 15$. Largest population transfer is achieved for $\omega_{\text{drive}} = \Delta\omega$.

3.3 Quantum Collectiveness

It would superficially appear that quantum collective behavior is closely linked with multi–body entanglement. To that end, one would ideally want a measure of collectivity, similar to one of the many proposed measures of entanglement. We believe the essence of quantum collective behavior is the emergent structure they induce, and the resultant cooperative enhancement of more fundamental properties. To elucidate the connection between collectiveness and multi–body entaglement, we consider the simplest case of two spins in the presence of an electromagnetic field and dipolar interaction

$$\hat{\mathcal{H}} = \frac{\omega}{2}\hat{\sigma}_z^1 + \frac{\omega}{2}\hat{\sigma}_z^2 + \frac{\Omega}{2}\left(\hat{\sigma}_+^1\hat{\sigma}_-^2 + \hat{\sigma}_-^1\hat{\sigma}_+^2\right). \tag{3.15}$$

The eigenstructure is then just the "collective" states of the two spins

$$|g\rangle = |\downarrow\downarrow\rangle\,, \tag{3.16}$$

$$|s\rangle = \frac{1}{\sqrt{2}}\left(|\uparrow\downarrow\rangle + |\downarrow\uparrow\rangle\right), \tag{3.17}$$

$$|a\rangle = \frac{1}{\sqrt{2}}\left(|\uparrow\downarrow\rangle - |\downarrow\uparrow\rangle\right), \tag{3.18}$$

$$|e\rangle = |\uparrow\uparrow\rangle\,. \tag{3.19}$$

With energies, $-\omega, \Omega, -\Omega, \omega$ respectively. Notice that the symmetric and anti–symmetric states are the maximally entangled Bell states. In the basis defined by (3.16), (3.17), (3.18), and (3.19) the two–spin system acts as a single four level system. We also know that in the Dicke model [19] that the symmetric state decay channel $|e\rangle \to |s\rangle \to |g\rangle$ is the enhanced collective behaviour known as superradiance, while $|e\rangle \to |a\rangle \to |g\rangle$ is a subradiant transition. One then wonders if all the eigenstates (3.16), (3.17), (3.18), and (3.19) in which the two spins act as one larger four level system are collective, or just the symmetric and anti–symmetric states for which non–classical effects can be seen. If we choose the former, then we notice that while the maximally entangled states $|s\rangle$ and $|a\rangle$ are collective, the separable states $|g\rangle$ and $|e\rangle$ are also collective in this case and thus discriminating between entangled and separable states is not akin to discriminating between collective and non–collective states.

Sensitivity to Coherent Operations as a Measure of Collectiveness

Some methods have been suggested as to measure collectiveness of which the most promising is the permutation symmetric method [24]. Another possible measure of collectiveness for an ensemble might be to determine how sensitive the collection is to erroneous

perturbative coherent operations. The most sensitive stand–alone states have been shown in [25], however, it is likely that due to degeneracy factors increasing the erroneous action, the most sensitive *subspace* would likely be more near j^* for ensemble systems such as the one considered here. In this way, this would provide a measure of sorts of the level of collectiveness of the various angular momentum subspaces.

If we wish to simply categorize whether a particular state is collective or not, we might follow a protocol for the discrimination between collective and non–collective states utilizing quantum Fisher information. For example, a quantum state $\hat{\rho}$, of a system of spin–1/2 particles are collective if after a unitary transformation $\hat{\rho} \to \hat{\rho}_\theta = e^{i\theta \hat{J}_{\vec{n}}} \hat{\rho} e^{-i\theta \hat{J}_{\vec{n}}}$, there exists an optimal collective POVM measurement μ such that uncertainty in the phase estimation $\Delta\theta_{\text{est}}$ saturates the Cramér–Rao bound. The sensitivity of the phase estimator is bounded by the Cramér–Rao bound [29]

$$\Delta\theta_{\text{est}} \geq \frac{1}{\sqrt{nF_Q}}, \tag{3.20}$$

where n is the number of times the measurement is repeated and F_Q is the quantum Fisher information. The quantum Fisher information of a state $\hat{\rho}$ with respect to an observable $\hat{A}$ is given by [52]

$$F_Q[\hat{\rho}, \hat{A}] = 2 \sum_{l,k} \frac{(\lambda_k - \lambda_l)^2}{(\lambda_k + \lambda_l)} |\langle k|\hat{A}|l\rangle|^2. \tag{3.21}$$

Given a collective observable, the Fisher information may prove to be a valuable measure for how much information $\hat{\rho}$ stores in its collective degrees of freedom. For the case of a pure state $|\psi\rangle$ and transformation generated the collective spin operators $\{\hat{J}_x, \hat{J}_y, \hat{J}_z\}$ we have that [10]

$$F_Q[|\psi\rangle, \hat{J}_{\vec{n}}] = 4\langle(\Delta \hat{J}_{\vec{n}})^2\rangle. \tag{3.22}$$

Maximizing Fisher information F_Q is reduced to finding the optimal direction $\vec{n}$. For example, the cat state saturates this bound. The collective correlation matrix C for a quantum state $\hat{\rho}$ is defined by the matrix elements

$$C_{ij} = \frac{1}{2}\langle \hat{J}_i \hat{J}_j + \hat{J}_j \hat{J}_j \rangle - \langle \hat{J}_i \rangle \langle \hat{J}_j \rangle, \tag{3.23}$$

where $\langle \hat{A} \rangle = \text{tr}\left(\hat{\rho}\hat{A}\right)$.

Then the maximum Fisher information is the maximum eigenvalue of the collective correlation matrix C. This follows from the fact that $F_Q = 4\langle(\Delta \hat{J}_{\vec{n}})^2\rangle = 4\langle n|C|n\rangle$.

Given the relation between the Fisher information and collective correlation matrix C, we can define a metric on the space of collective matrices as follows [52]:

$$\delta(P,Q) = \sqrt{\operatorname{tr} P + \operatorname{tr} Q - 2\,\mathrm{F}(P,Q)}, \tag{3.24}$$

where P, Q are any positive semi–definite matrices and $\mathrm{F}(P,Q) = \left[\operatorname{tr}\sqrt{\sqrt{P}Q\sqrt{P}}\right]^2$ is the fidelity. Not only can we discriminate between collective and non–collective states but we can measure how close states are under our definition of "collective–ness" by first calculating the collective correlation matrix C and using the metric δ.

Chapter 4

Conclusion and Future Directions

Cavity QED has garnered great interest in recent years for it's versatile use in quantum information. The main system of interest in this text is the Tavis–Cummings system, which can be realized by many different experiments, electronic spin resonance (ESR), nuclear magnetic resonance (NMR), NV centers, superconducting qubits, and neutral atoms. In a typical ESR experiment the ensemble of spins can contain 10^3 and up to 10^{18} identical spins. Describing such a system becomes impossible, since Tavis–Cummings model does not admit exact solutions for arbitrary number of TLS. Meanwhile, simulating the system is also impossible due to the exponential growth of hardness in the number of TLS. However, using the techniques introduced in this text, we can gain interesting insights into the structure of the Hamiltonian that can aid in both producing significantly more efficient numerical simulations and derive values critical to the design of spin–cavity experimental setups. First, we showed that by considering an extra good quantum number, the total angular–momentum, we can rewrite our Hamiltonian in a new basis that is agnostic to the degeneracy of each total angular–momentum subspace, effectively reducing the complexity of our system from exponential (2^N) to quadratic (N^2) in the number of TLS (N). In addition, by noticing that most of the population resides in the first $\mathrm{O}(\sqrt{N})$ angular–momentum subspaces, we can further reduce the complexity by approximating the system with only the first $\mathrm{O}(\sqrt{N})$ subspaces. With efficient techniques for calculating the energy of the Tavis–Cummings model, we introduced a better bound on the validity of the strong–coupling regime and the rotating wave approximation. These methods can be used to justify experimental setups and aid in the development of new quantum information techniques, by way of better spin–cavity control [1, 54, 55]. This thesis has only been concerned with systems with low temperatures T, as such an interesting research direction is a more nuanced treatment of the thermal behaviour of the Tavis–Cumming model. An-

other, future research directions in is a full description of quantum collectiveness especially as they pertain to spin–cavity systems. Such a description would be critical to extracting information from quantum systems.

References

[1] Bartolo Albanese, Sebastian Probst, Vishal Ranjan, Christoph W Zollitsch, Marek Pechal, Andreas Wallraff, John JL Morton, Denis Vion, Daniel Esteve, Emmanuel Flurin, et al. Radiative cooling of a spin ensemble. *Nature Physics*, pages 1–5, 2020.

[2] Victor V Albert and Liang Jiang. Symmetries and conserved quantities in lindblad master equations. *Physical Review A*, 89(2):022118, 2014.

[3] Ben Q Baragiola, Bradley A Chase, and JM Geremia. Collective uncertainty in partially polarized and partially decohered spin-1 2 systems. *Physical Review A*, 81(3):032104, 2010.

[4] W Barth, RS Martin, and JH Wilkinson. Calculation of the eigenvalues of a symmetric tridiagonal matrix by the method of bisection. *Numerische Mathematik*, 9(5):386–393, 1967.

[5] MA Bastarrachea-Magnani, S Lerma-Hernández, and JG Hirsch. Comparative quantum and semiclassical analysis of atom-field systems. ii. chaos and regularity. *Physical Review A*, 89(3):032102, 2014.

[6] Rodney J Baxter. *Exactly solved models in statistical mechanics*. Elsevier, 2016.

[7] NM Bogoliubov, RK Bullough, and J Timonen. Exact solution of generalized tavis-cummings models in quantum optics. *Journal of Physics A: Mathematical and General*, 29(19):6305, 1996.

[8] NM Bogolyubov. Algebraic bethe anzatz and the tavis-cummings model. *Journal of Mathematical Sciences*, 100(2):2051–2060, 2000.

[9] Daniel Braak. Integrability of the rabi model. *Physical Review Letters*, 107(10):100401, 2011.

[10] Samuel L Braunstein, Carlton M Caves, and Gerard J Milburn. Generalized uncertainty relations: theory, examples, and lorentz invariance. *annals of physics*, 247(1):135–173, 1996.

[11] Heinz-Peter Breuer, Francesco Petruccione, et al. *The theory of open quantum systems*. Oxford University Press on Demand, 2002.

[12] M Brune, P Nussenzveig, F Schmidt-Kaler, F Bernardot, Abdelhamid Maali, JM Raimond, and S Haroche. From lamb shift to light shifts: Vacuum and subphoton cavity fields measured by atomic phase sensitive detection. *Physical review letters*, 72(21):3339, 1994.

[13] Bradley A Chase and JM Geremia. Collective processes of an ensemble of spin-1/ 2 particles. *Physical Review A*, 78(5):052101, 2008.

[14] Qing-Hu Chen, Tao Liu, Yu-Yu Zhang, and Ke-Lin Wang. Exact solutions to the jaynes-cummings model without the rotating-wave approximation. *EPL (Europhysics Letters)*, 96(1):14003, 2011.

[15] Ed S Coakley and Vladimir Rokhlin. A fast divide-and-conquer algorithm for computing the spectra of real symmetric tridiagonal matrices. *Applied and Computational Harmonic Analysis*, 34(3):379–414, 2013.

[16] Thomas L Curtright, David B Fairlie, Cosmas K Zachos, et al. A compact formula for rotations as spin matrix polynomials. *SIGMA. Symmetry, Integrability and Geometry: Methods and Applications*, 10:084, 2014.

[17] Carlos M da Fonseca. On the location of the eigenvalues of jacobi matrices. *Applied mathematics letters*, 19(11):1168–1174, 2006.

[18] MAM De Aguiar, K Furuya, CH Lewenkopf, and MC Nemes. Chaos in a spin-boson system: Classical analysis. *Annals of Physics*, 216(2):291–312, 1992.

[19] Robert H Dicke. Coherence in spontaneous radiation processes. *Physical review*, 93(1):99, 1954.

[20] JM Fink, R Bianchetti, Matthias Baur, M Göppl, Lars Steffen, Stefan Filipp, Peter J Leek, Alexandre Blais, and Andreas Wallraff. Dressed collective qubit states and the tavis-cummings model in circuit qed. *Physical review letters*, 103(8):083601, 2009.

[21] JM Fink, R Bianchetti, Matthias Baur, M Göppl, Lars Steffen, Stefan Filipp, Peter J Leek, Alexandre Blais, and Andreas Wallraff. Dressed collective qubit states and the tavis-cummings model in circuit qed. *Physical review letters*, 103(8):083601, 2009.

[22] JM Fink, M Göppl, M Baur, R Bianchetti, PJ Leek, Alexandre Blais, and Andreas Wallraff. Climbing the jaynes–cummings ladder and observing its nonlinearity in a cavity qed system. *Nature*, 454(7202):315–318, 2008.

[23] Barry M Garraway. The dicke model in quantum optics: Dicke model revisited. *Philosophical Transactions of the Royal Society A: Mathematical, Physical and Engineering Sciences*, 369(1939):1137–1155, 2011.

[24] Michael Gegg, Alexander Carmele, Andreas Knorr, and Marten Richter. Superradiant to subradiant phase transition in the open system dicke model: Dark state cascades. *New Journal of Physics*, 20(1):013006, 2018.

[25] Daniel Gottesman. Maximally sensitive sets of states. *arXiv preprint arXiv:1907.05950*, 2019.

[26] Martin C Gutzwiller. *Chaos in classical and quantum mechanics*, volume 1. Springer Science & Business Media, 2013.

[27] Klemens Hammerer, Anders S Sørensen, and Eugene S Polzik. Quantum interface between light and atomic ensembles. *Reviews of Modern Physics*, 82(2):1041, 2010.

[28] Serge Haroche and Jean-Michel Raimond. *Exploring the Quantum*. Oxford University Press, 2006.

[29] Carl W Helstrom and Carl W Helstrom. *Quantum detection and estimation theory*, volume 3. Academic press New York, 1976.

[30] Edwin T Jaynes and Frederick W Cummings. Comparison of quantum and semiclassical radiation theories with application to the beam maser. *Proceedings of the IEEE*, 51(1):89–109, 1963.

[31] BR Judd. Exact solutions to a class of jahn-teller systems. *Journal of Physics C: Solid State Physics*, 12(9):1685, 1979.

[32] Anton Frisk Kockum, Adam Miranowicz, Simone De Liberato, Salvatore Savasta, and Franco Nori. Ultrastrong coupling between light and matter. *Nature Reviews Physics*, 1(1):19–40, 2019.

[33] Jongmin Lee, Michael J Martin, Yuan-Yu Jau, Tyler Keating, Ivan H Deutsch, and Grant W Biedermann. Demonstration of the jaynes-cummings ladder with rydberg-dressed atoms. *Physical Review A*, 95(4):041801, 2017.

[34] Andrzej J Maciejewski, Maria Przybylska, and Tomasz Stachowiak. Full spectrum of the rabi model. *Physics Letters A*, 378(1-2):16–20, 2014.

[35] Johannes Majer, JM Chow, JM Gambetta, Jens Koch, BR Johnson, JA Schreier, L Frunzio, DI Schuster, Andrew Addison Houck, Andreas Wallraff, et al. Coupling superconducting qubits via a cavity bus. *Nature*, 449(7161):443–447, 2007.

[36] Harold J Metcalf and Peter Van der Straten. Laser cooling and trapping of neutral atoms. *The Optics Encyclopedia: Basic Foundations and Practical Applications*, 2007.

[37] Silvia Noschese, Lionello Pasquini, and Lothar Reichel. Tridiagonal toeplitz matrices: properties and novel applications. *Numerical linear algebra with applications*, 20(2):302–326, 2013.

[38] MD Reed, L DiCarlo, BR Johnson, L Sun, DI Schuster, L Frunzio, and RJ Schoelkopf. High-fidelity readout in circuit quantum electrodynamics using the jaynes-cummings nonlinearity. *Physical review letters*, 105(17):173601, 2010.

[39] BC Rose, AM Tyryshkin, H Riemann, NV Abrosimov, P Becker, H-J Pohl, MLW Thewalt, Kohei M Itoh, and SA Lyon. Coherent rabi dynamics of a superradiant spin ensemble in a microwave cavity. *Physical Review X*, 7(3):031002, 2017.

[40] Heinz Rutishauser. The jacobi method for real symmetric matrices. *Numerische Mathematik*, 9(1):1–10, 1966.

[41] Jun John Sakurai and Eugene D Commins. Modern quantum mechanics, revised edition, 1995.

[42] DI Schuster, AP Sears, E Ginossar, L DiCarlo, L Frunzio, JJL Morton, H Wu, GAD Briggs, BB Buckley, DD Awschalom, et al. High-cooperativity coupling of electron-spin ensembles to superconducting cavities. *Physical review letters*, 105(14):140501, 2010.

[43] Marlan O Scully and M Suhail Zubairy. Quantum optics, 1999.

[44] Bruce W Shore and Peter L Knight. The jaynes-cummings model. *Journal of Modern Optics*, 40(7):1195–1238, 1993.

[45] Richard P Stanley. Algebraic combinatorics. *Springer*, 20:22, 2013.

[46] Andrew Stasiuk, Lane G Gunderman, Mohamed El Mandouh, Troy W Borneman, and David G Cory. Generalized collective lamb shift. *arXiv preprint arXiv:2101.09550*, 2021.

[47] Michael Tavis and Frederick W Cummings. Exact solution for an n-molecule—radiation-field hamiltonian. *Physical Review*, 170(2):379, 1968.

[48] Gerald Teschl. *Jacobi operators and completely integrable nonlinear lattices*. Number 72. American Mathematical Soc., 2000.

[49] JJ Viennot, MC Dartiailh, Audrey Cottet, and Takis Kontos. Coherent coupling of a single spin to microwave cavity photons. *Science*, 349(6246):408–411, 2015.

[50] Yimin Wang and Jing Yan Haw. Bridging the gap between the jaynes–cummings and rabi models using an intermediate rotating wave approximation. *Physics Letters A*, 379(8):779–786, 2015.

[51] David S Watkins. Product eigenvalue problems. *SIAM review*, 47(1):3–40, 2005.

[52] John Watrous. *The Theory of Quantum Information*. Cambridge University Press, 2018.

[53] Janus Wesenberg and Klaus Mølmer. Mixed collective states of many spins. *Physical Review A*, 65(6):062304, 2002.

[54] Christopher J Wood, Troy W Borneman, and David G Cory. Cavity cooling of an ensemble spin system. *Physical Review Letters*, 112(5):050501, 2014.

[55] Christopher J Wood and David G Cory. Cavity cooling to the ground state of an ensemble quantum system. *Physical Review A*, 93(2):023414, 2016.

[56] Honghua Zhong, Qiongtao Xie, Murray T Batchelor, and Chaohong Lee. Analytical eigenstates for the quantum rabi model. *Journal of Physics A: Mathematical and Theoretical*, 46(41):415302, 2013.

APPENDICES

Appendix A

The Rotating Wave Approximation

Beginning with the full Hamiltonian describing the Jaynes–Cummings model without the rotating wave approximation (1.1.1)

$$\hat{\mathcal{H}} = \frac{\omega_{\text{tls}}}{2}\hat{\sigma}_z + \omega_{\text{c}}\hat{a}^\dagger\hat{a} + g(\hat{\sigma}_+ + \hat{\sigma}_-)(\hat{a}^\dagger + \hat{a}). \tag{A.1}$$

Taking a small step back, we know that the time–evolution of an operator in the Heisenberg picture is given by

$$\frac{d\hat{A}}{dt} = i\Big[\hat{\mathcal{H}}, \hat{A}\Big], \tag{A.2}$$

then for the cavity annihilation operator $\hat{a}$ we have

$$\begin{aligned}
\frac{d\hat{a}}{dt} &= i\Big[\hat{\mathcal{H}}, \hat{a}\Big] && \text{(A.3)}\\
&= i\big[\omega_{\text{c}}\hat{a}^\dagger\hat{a}, \hat{a}\big] && \text{(A.4)}\\
&= -i\omega_{\text{c}}\hat{a}, && \text{(A.5)}
\end{aligned}$$

hence the time–dependent solution of the annihilation operator is

$$\hat{a}(t) = \hat{a}(0)e^{-i\omega_{\text{c}}t}, \tag{A.6}$$

thus we also have

$$\hat{a}^\dagger(t) = \hat{a}^\dagger(0)e^{i\omega_{\text{c}}t}. \tag{A.7}$$

Similarly, the time–dependent equation for the TLS raising and lower operators are

$$\hat{\sigma}_+(t) = \hat{\sigma}_+(0)e^{i\omega_{\rm tls}t} \tag{A.8}$$

$$\hat{\sigma}_-(t) = \hat{\sigma}_-(0)e^{-i\omega_{\rm tls}t}. \tag{A.9}$$

To that end, we can rewrite the interaction term with explicit time–dependence

$$\hat{\mathcal{H}}_{\rm int}(t) = g(\hat{\sigma}_+(0)e^{i\omega_{\rm tls}t} + \hat{\sigma}_-(0)e^{-i\omega_{\rm tls}t})(\hat{a}^\dagger(0)e^{i\omega_{\rm c}t} + \hat{a}(0)e^{-i\omega_{\rm c}t}). \tag{A.10}$$

Consider the change of basis to the interaction picture given by

$$\hat{U} = \exp\Big[i\hat{\mathcal{H}}_0 t\Big], \tag{A.11}$$

where $\hat{\mathcal{H}}_0 = \frac{\omega_{\rm tls}}{2}\hat{\sigma}_z + \omega_{\rm c}\hat{a}^\dagger\hat{a}$ is the bare TLS and cavity Hamiltonian. Then the full Jaynes–Cummings Hamiltonian (A.1) in the interaction picture is given by

$$\hat{\mathcal{H}}_{\rm rot} = g(\hat{\sigma}_+\hat{a}e^{-i(\omega_{\rm tls}-\omega_{\rm c})t} + \hat{\sigma}_-\hat{a}^\dagger e^{i(\omega_{\rm tls}-\omega_{\rm c})t}) + g(\hat{\sigma}_+\hat{a}^\dagger e^{i(\omega_{\rm tls}+\omega_{\rm c})t} + \hat{\sigma}_-\hat{a}e^{-i(\omega_{\rm tls}+\omega_{\rm c})t}), \tag{A.12}$$

where we set $\hat{a} \equiv \hat{a}(0)$ and $\hat{\sigma}_- \equiv \hat{\sigma}(0)$ for brevity. The first term with slowly oscillating components $(\omega_{\rm tls} - \omega_{\rm c})$ in (A.12) is referred to as the "co–rotating" term, while the second term with the fast oscillating components $(\omega_{\rm tls} + \omega_{\rm c})$ is referred to as the "counter–rotating" term. In the cases where the counter–rotating term is dropped, it is termed the *rotating wave approximation*. In the case of the Jaynes–Cummings model, the counter–rotating term can be ignored when the coupling strength g between the TLS and cavity is much smaller than the effective frequency, such that the influence counter–rotating term on the dynamics of the system is very small. In addition, the validity of the rotating wave approximation depends on the temperature of the system. In the case where of high temperatures T, excitation and spin numbers are no longer good quantum numbers and rotating wave approximation breaks down. However, in this thesis regimes of high temperatures are not considered. Thus, we always assume that the system is cold enough such that rotating wave approximation holds.